Size-Dependent Hydrogen Bonds of Cluster Ions between Phenol Cation Radicals and Water Molecules: A Molecular Orbital Study

Suyong Re and Yoshihiro Osamura*

Department of Chemistry, Faculty of Science, Rikkyo University, 3-34-1 Nishi-ikebukuro, Toshima-ku, Tokyo 171-8501, Japan

Received: December 9, 1997; In Final Form: March 13, 1998

The molecular structures and vibrational frequencies of $[C_6H_5OH-(H_2O)_n]^{\bullet+}$ ($n = 1-4$) are studied by employing ab initio molecular orbital methods. Since the hydrogen bond between phenol cation radicals and water molecules is much stronger than that of the neutral phenol−water system, the position of the proton of phenol cation radicals depends on the number of water molecules in the clusters $[C_6H_5OH-(H_2O)_n]^{\bullet+}$. Although the stable structure of $[C_6H_5OH-(H_2O)_n]^{\bullet+}$ varies depending on the method used in the calculation, the result obtained with the B3LYP density functional method gives good agreement with the experimental IR spectra. The proton-nontransferred form is found to be most stable for $n = 1$ and $n = 2$ clusters. In the cases of $n \geq 3$, the most stable structures are the proton-transferred form. There are two types of structures obtained for $n = 3$ clusters, where the branched form is more stable than the chained form. The optimized structures for $n = 3$ and $n = 4$ clusters show that the H_3O^+ moiety prefers to interact with the phenoxy radical and two water molecules.

I. Introduction

Phenol−water clusters and their ions are of increasing interest from both experimental and theoretical points of view. This cluster system is one of the molecular model systems of solute−solvent interaction involving hydrogen bonds in the condensed phase. The intracluster proton-transfer process in this system is also interesting in conjunction with acid−base reactions in aqueous solutions of organic molecules.

The recent series of spectroscopic studies on the phenol−water clusters revealed that there is a significant difference in the structures between neutral hydrogen-bonded clusters and their ionized clusters.[1−9] While the interaction between phenol and water clusters is not strong enough to dissociate the proton of phenol, the phenol−water cluster ions have the proton-transferred form by increasing the number of water molecules. Evidence for this is demonstrated by using infrared multiphoton dissociation spectroscopy combined with an ion-trapping technique named trapped ion photodissociation (TIP) spectroscopy.[7−9] By TIP spectroscopy, Mikami et al. observed the infrared spectra of the OH stretching vibration bands for the phenol−water cluster cations $[C_6H_5OH-(H_2O)_n]^{\bullet+}$ ($n = 1-4$). They have concluded that the $n = 1$ and 2 cluster ions have the proton-nontransferred form and the cluster ions $n \geq 3$ have the proton-transferred form from both their electronic and OH vibrational spectra.[7,8]

The proton-transferred form is also observed for phenol−ammonia cluster ions.[9−11] In the case of $[C_6H_5OH-NH_3]^{\bullet+}$, analysis of the mass spectroscopy indicates that there are two peaks of the ions $C_6H_5OH^{\bullet+}$ and parent ion $[C_6H_5OH-NH_3]^+$ after photoionization,[12] while the TIP spectrum shows only the NH_4^+ ion.[9,11] This experimental evidence suggests that there are two energy minima for the $[C_6H_5OH-NH_3]^{\bullet+}$ cluster.[9,10] While the cluster ions generated by vertical ionization have not been proton-transferred yet, the cluster ions may stabilize to a proton-transferred structure after energy relaxation.

In the case of C_6H_5OH−water cluster ions, Mikami speculated that the potential energy surfaces have double energy minima along the proton-transfer reaction.[1,7,8] Since the electronic and IR spectra observed by the ion-trapped experiment only give information after relaxation, there are several remaining questions not only on the potential energy surface of the proton transfer but also on the geometrical structure of the ion clusters as well as their spectroscopic assignment.

One of the advantages of using quantum chemical methods is to explore the detailed geometrical information and the potential energy surfaces. To obtain these details, we have carried out ab initio molecular orbital calculations on the $[C_6H_5OH-(H_2O)_n]^{\bullet+}$ ($n = 1-4$) and $[C_6H_5OH-NH_3]^{\bullet+}$ clusters. We have calculated the equilibrium structures of several most probable cluster ions in order to clarify the size dependency on the proton transfer.

II. Computational Methods

The geometries of the $[C_6H_5OH-(H_2O)_n]^{\bullet+}$ ($n = 1-4$) and $[C_6H_5OH-NH_3]^{\bullet+}$ systems have been optimized using three different molecular orbital methods. The Hartree−Fock (HF) method gives a qualitatively reasonable result for the molecular structure in most cases. Since the HF method does not include the effect of electron correlation, the naive system such as the system involving hydrogen bonds must be confirmed by using other methods. We have employed the second-order Møller−Plesset perturbation method (MP2)[13] in order to include the dynamical electron correlation for valence electrons. We have also used the hybrid density functional B3LYP method,[14,15] which is the Becke's three-parameter nonlocal-exchange functional of Lee, Yang, and Parr.[16] The density functional method,[17] especially the B3LYP method, is recently used for various systems and gives very promising results for many molecular systems. We have used the double-ζ plus polarization (DZP) basis set[18,19] in all calculations. The vibrational analyses have been carried out by using the analytical second derivative

S1089-5639(98)00468-X CCC: $15.00
Published on Web 05/05/1998

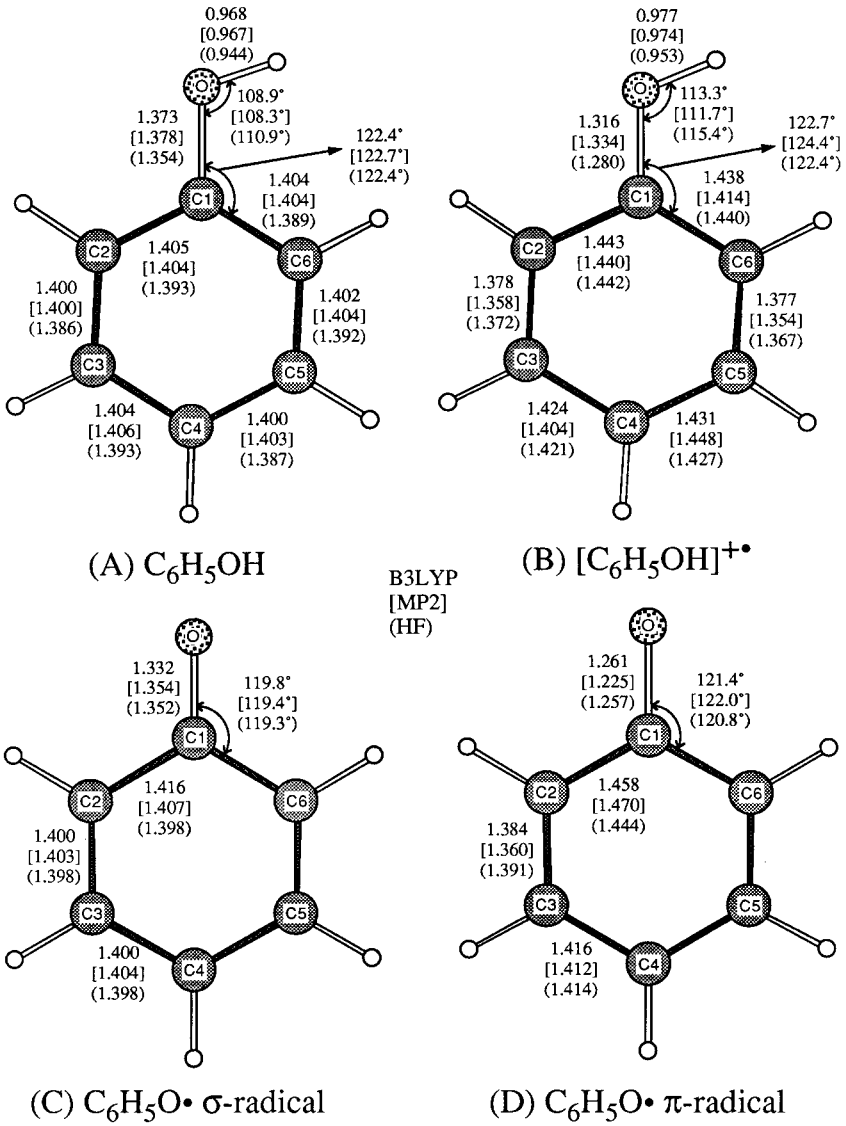

Figure 1. Optimized structures of phenol (A), phenol cation radical (B), and phenoxy radicals (C, D) by using the B3LYP method with the DZP basis set. The bond lengths are shown in Å. The values shown in the square brackets [ ] are obtained with the MP2/DZP method. The values shown in the parentheses ( ) are obtained with the HF/DZP method.

method for all optimized geometries. The calculated values of the relative energies stated in the text are the noncorrected values of the zero-point vibrational energies without any specification, since the global feature of the potential energy surface does not change by the correction of the zero-point vibrational energies. The calculated values of proton affinity (PA) are the corrected values of the zero-point vibrational energies. To examine the effect of the basis set superposition error (BSSE) for these systems, we have evaluated the BSSE at the optimized geometries for only small size clusters, such as the neutral $[C_6H_5OH-H_2O]$ and $[C_6H_5OH-NH_3]$ and ion $[C_6H_5OH-H_2O]^{\bullet+}$ clusters by using the counterpoise method.[20] The obtained value of BSSE is ca. 1 kcal/mol for both the neutral and ion clusters of phenol−water system and ca. 5 kcal/mol for the phenol−ammonia cluster. Since there is no significant effect on the potential energy surfaces, we will discuss in the text, the energies without the BSSE correction. All calculations have been carried out with the GAUSSIAN 94 program package.[21]

III. Results and Discussion

A. Phenol and Its Cation Radical. Before we discuss the structures of phenol−water cluster ions, we have to check the validity of the computational methods not only on the structures but also on the vibrational frequencies for the system, which has been well-characterized. Since all of the vibrational frequencies of phenol were assigned experimentally,[22−25] we may judge the accuracy of the theoretical methods by comparing the theoretically calculated values with the experimental ones. Two papers have been recently published on the theoretical calculations of the vibrational frequencies of phenol by using the density functional method.[26,27] These studies indicate that the hybrid density functional B3LYP method gives very reasonable frequencies for the phenol molecule.

Figure 1 illustrates the optimized structures of phenol (A) and its cation radical (B) calculated with the HF, MP2, and B3LYP methods by using the DZP basis set. The largest difference of the geometries of phenol obtained with the HF, MP2, and B3LYP methods is 0.024 Å in the C−O bond length. The experimental geometry of phenol in the gas phase[28] agrees well with the averaged geometry of the HF and B3LYP optimized structures. While all C−C bonds are almost equivalent (1.4 Å) in phenol, the structure of the phenol cation radical is distorted toward the quinoidal form because of an electron loss from the HOMO (highest occupied molecular orbital) of

TABLE 1: Vibrational Frequencies (cm^{-1}) of Phenol and Its Cation Radical Calculated by Using the MP2 and B3LYP Methods with the DZP Basis Set

			phenol				phenol$^{\bullet+}$	
mode[a]			expt[b]	HF	MP2	B3LYP	HF	MP2	B3LYP
In-Plane (a′)									
a_1	1	OH str.	*3657*[d]	4210	3891	3845	4082	3805	3732
	2	CH str. (20a)	*3087*[d]	3398	3287	3217	3421	3322	3239
	3	CH str. (2)	*3063 (3075*[d]*)*	3365	3254	3185	3404	3302	3227
	4	CH str. (13)	*3027*	3347	3237	3166	3387	3283	3203
	5	CC str. (8a)	*1603 (1610*[c,e]*)*	1799	1676	1655	1774	1950	1657
	6	CC str. (19a)	*1501*	1657	1542	1524	1512	1425	1387
	7	CO str. (7a)	*1262*[e]	1396	1300	1288	1589	1519	1504
	8	OH bend	*1177*	1285	1211	1190	1142	1177	1097
	9	CH bend (9a)	*1169*	1275	1199	1183	1262	1243	1198
	10	CH bend (18a)	*1026*[e]	1114	1046	1037	1016	1019	982
	11	ring (1)	*999*[e]	1075	1013	1000	1058	986	988
	12	ring (12)	*823*	885	825	823	861	826	813
	13	ring (6a)	*527*	570	528	529	548	563	519
b_2	1	CH str. (20b)	*3070*	3390	3280	3209	3416	3312	3233
	2	CH str. (7b)	*3049*	3375	3265	3194	3410	3295	3219
	3	CC str. (8b)	*1610 (1603*[c, e]*)*	1786	1663	1641	1637	1677	1536
	4	CC str. (19b)	*1472*	1622	1508	1495	1554	1479	1445
	5	CC str. (14)	*1343*	1366	1475	1370	1487	1399	1412
	6	CH bend (3)	*1277*	1479	1369	1354	1446	1373	1357
	7	CH bend (9b)	*1151*	1187	1184	1171	1267	1206	1185
	8	CH bend (15)	*1072*	1169	1098	1088	1210	1070	1141
	9	ring (6b)	*619*	672	622	623	586	478	562
	10	CO bend (18b)	*403*	439	402	404	455	334	412
Out-of-Plane (a″)									
b_1	1	CH bend (5)	*973*	1100	898	982	1038	1043	994
	2	CH bend (17b)	*881*	984	825	883	955	994	937
	3	CH bend (10b)	*751*	841	725	761	861	826	813
	4	CC twist (4)	*686*	762	630	698	669	609	623
	5	ring (16b)	*503*	562	494	513	474	424	435
	6	OH torsion	*309*	305	311	339	676	571	607
	7	ring (11)	*245*	251	222	229	186	191	184
a_2	1	CH bend (17a)	*995 (958*[c,d]*)*	1081	875	959	1055	1064	1008
	2	CH bend (10a)	*817*	915	787	819	834	874	804
	3	CC twist (16a)	*409*	455	403	417	374	381	359

[a] Each vibrational mode is assigned based on the Wilson's indices shown in parentheses under the C_{2v} symmetry, although phenol has C_s symmetry. [b] The experimental frequencies are taken from ref 22, otherwise indicated as: [c] Reference 23. [d] Reference 24. [e] Reference 25.

phenol. The positive charge of the phenol cation radical is distributed on the phenyl ring owing to the π radical character. We can observe the shortening of the C−O bond and the elongation of the O−H bond caused by ionization. These structural changes yield frequency shifts of the C−O and O−H stretching vibrations and the increase of acidity of ionized phenol. The geometry of the phenol cation radical obtained with the MP2 method somewhat differs from those calculated with the HF and B3LYP methods.

Table 1 summarizes the vibrational frequencies of phenol calculated with several methods. Although the HF method always overestimates the vibrational frequencies more than 10% compared to the experimental values, the inclusion of dynamical electron correlation such as the MP2 method improves the frequency values within the error of 10%. The MP2 method, however, tends to underestimate the frequencies of the out-of-plane modes. The B3LYP method gives very good agreement with the experimental values despite the fact that the calculated frequencies are evaluated with harmonic approximation. The difference between the experimental values and the calculated values with the B3LYP method is found to be less than 6% except for the OH torsional mode. The present B3LYP calculation with the DZP basis set gives better agreement with the experimental frequencies than the previously reported B3LYP calculation with the 6-31G** basis set.[26,27]

Table 1 also shows the calculated frequencies of the phenol cation radical. There are no experimental vibrational frequencies of the phenol cation radical except for the OH stretching, 3535 cm^{-1}.[29] The calculated values of the OH frequency clearly show the red-shift of 100 cm^{-1} caused by the ionization of phenol. The change of the C−O stretching frequency is more remarkable than that of the O−H vibration and is calculated to be over 200 cm^{-1} blue shifted.

Since the MP2 method sometimes overestimates the effect of electron correlation, the result obtained with the B3LYP method seems to be reasonable to describe not only the molecular structure but also the vibrational frequencies of cation radical species.

B. Molecular Structure and Vibrational Frequencies of the Phenoxy Radical. We have also calculated the structure and vibrational frequencies of the phenoxy radical $C_6H_5O^{\bullet}$, which is a deprotonated species of the phenol cation radical. The structure and vibrational frequencies of the phenoxy radical have been studied both experimentally[30−32] and theoretically.[33−35] As phenol cation is in the π radical state, the ground state of the phenoxy radical is the $^2B_1$ π radical state. Note, however, that there is a very low-lying excited state of phenoxy radical, which is the $^2B_2$ σ radical state.

The second row of Figure 1 depicts the optimized structures of the phenoxy radical in both π and σ radical states (Figure 1 (C and D)). The geometry of the ground state of the phenoxy radical is similar to that of the phenol cation radical. The geometrical analogy can also be found between neutral phenol and the phenoxy σ radical. The result obtained with the MCSCF

TABLE 2: Vibrational Frequencies of Phenoxy σ and π Radicals Calculated by Using the HF, MP2, and B3LYP Methods with the DZP Basis Set

			phenoxy π radical				phenoxy σ radical	
mode			expt	HF	MP2	B3LYP	HF	MP2	B3LYP
In-Plane (a′)									
a_1	1	CH str. (20a)		3396	3311	3221	3395	3291	3225
	2	CH str. (2)		3384	3300	3208	3383	3280	3214
	3	CH str. (13)		3364	3276	3186	3364	3254	3184
	4	CC str. (8a)	*1505*	1621	1715	1585	1714	1655	1615
	5	CC str. (19a)		1553	1543	1488	1617	1510	1449
	6	CO str. (7a)	*1398*	1402	1473	1410	1352	1281	1259
	7	CH bend (9a)	*1157*	1205	1186	1158	1250	1199	1184
	8	CH bend (18a)	*990*	1050	1038	1005	1084	1046	1039
	9	ring (1)		1024	973	970	1034	1006	980
	10	ring (12)	*840*	852	782	803	833	823	821
	11	ring (6a)	*528*	549	533	523	550	519	515
b_2	1	CH str. (20b)		3393	3308	3217	3389	3286	3223
	2	CH str. (7b)		3371	3283	3193	3372	3263	3189
	3	CC str. (8b)		1629	1632	1545	1675	1630	1587
	4	CC str. (19b)		1543	1469	1437	1560	1487	1449
	5	CC str. (14)		1423	1331	1345	1437	1435	1344
	6	CH bend (3)	*1331*	1391	1288	1278	1329	1328	1276
	7	CH bend (9b)		1224	1142	1159	1228	1187	1173
	8	CH bend (15)		1125	1128	1084	1142	1099	1087
	9	ring (6b)		631	594	590	655	616	614
	10	CO bend (18b)		475	457	441	401	365	367
Out-of-Plane (a″)									
b_1	1	CH bend (5)		997	1018	990	1038	897	970
	2	CH bend (17b)		919	937	918	932	826	869
	3	CH bend (10b)		796	829	798	787	720	725
	4	CC twist (4)		672	663	653	710	629	691
	5	ring (16b)		498	496	482	524	492	508
	6	ring (11)		211	174	190	249	227	226
a_2	1	CH bend (17a)		987	1017	977	1017	878	953
	2	CH bend (10a)		821	826	797	868	786	812
	3	CC twist (16a)		386	395	376	435	402	424

[a] The experimental frequencies are taken from ref 30.

method[33] gives similar tendency such that the phenoxy π radical has quinoidal structure while the σ radical has a regular hexagon structure. The bond distances, however, differ depending on the methods used. As Figure 1 shows, the MP2 method gives large geometrical difference between σ radical and the π radical, in particular on the C1−C2 and C2−C3 bond lengths, compared to the differences obtained with the HF and B3LYP methods.

Table 2 shows the vibrational frequencies of phenoxy radicals calculated with three different methods. Takahashi et al.[34] reported the good agreement between theoretical and experimental values of the frequencies of the phenoxy radical in the $^2B_1$ ground state, although only few frequencies are observed for the ground state of the phenoxy radical.[32] In the present study, similar results are obtained for the structure and vibrational frequencies of phenoxy π radical by using the B3LYP method. It is also found that the frequencies of the σ and π radicals well correspond to those of the neutral and cationic phenol, respectively.

The energy of the excited $^2B_2$ state (σ radical) is shown to be 47.8 kcal/mol above the ground state $^2B_1$ by the spectroscopic experiment.[31,32] The energy difference between these two states is calculated to be ca. 20 kcal/mol with the HF and B3LYP methods. The MP2 calculation, however, gives almost the same energies for these two states because of the overestimation of electron correlation effect for the σ radical state rather than the π radical state. The large difference between theoretical and experimental values must be refined by considering the multiconfiguration nature of the π radical state.

The HF calculation gives large spin contamination values $S^2 = 1.19$ and 1.39 for phenoxy σ and π radicals, respectively. The MP2 method reduces the value for the σ radical to 0.76, but gives 1.31 for the π radical. Excellent improvement of spin contamination (0.75 for the σ radical and 0.79 for the π radical) is obtained with the B3LYP method.

Consequently, the B3LYP method turns out to give the most reasonable result for not only the geometries but also the relative energies. In this respect, we will use the values calculated with the B3LYP method in the following discussions without any specification.

C. $C_6H_5OH-H_2O$ and $[C_6H_5OH-H_2O]^{\bullet+}$. Several authors studied the molecular structure and vibrational frequencies of the hydrogen-bonded complex between neutral phenol and the water molecule[25,36,37] as well as its cationic state.[38−40] In the neutral $[C_6H_5OH-H_2O]$ complex, phenol acts as a proton donor. Feller and Feyereisen[37] demonstrated that the hydrogen bond between the hydrogen of the water molecule and the oxygen atom of phenol is 3 kcal/mol less stable than that between the hydrogen of phenol and the oxygen of the water molecule at the MP2/6-31G** level of calculation.

The first row of Figure 2 shows the optimized structures of the hydrogen-bonded complexes for phenol (E) and its cation radical (F) obtained by using the HF, MP2, and B3LYP methods. All methods provide the proton-nontransferred form for both neutral and cation radical states of the hydrogen-bonded cluster of phenol with single water molecule. The geometry obtained for the cation radical complex agrees well with the previous theoretical studies that have shown that the $[C_6H_5OH-H_2O]^{\bullet+}$ cluster ion has the proton nontransferred structure.[39,41] The O−H bond of phenol in $[C_6H_5OH-H_2O]^{\bullet+}$ is calculated to be ca. 0.04 Å longer than that of the neutral

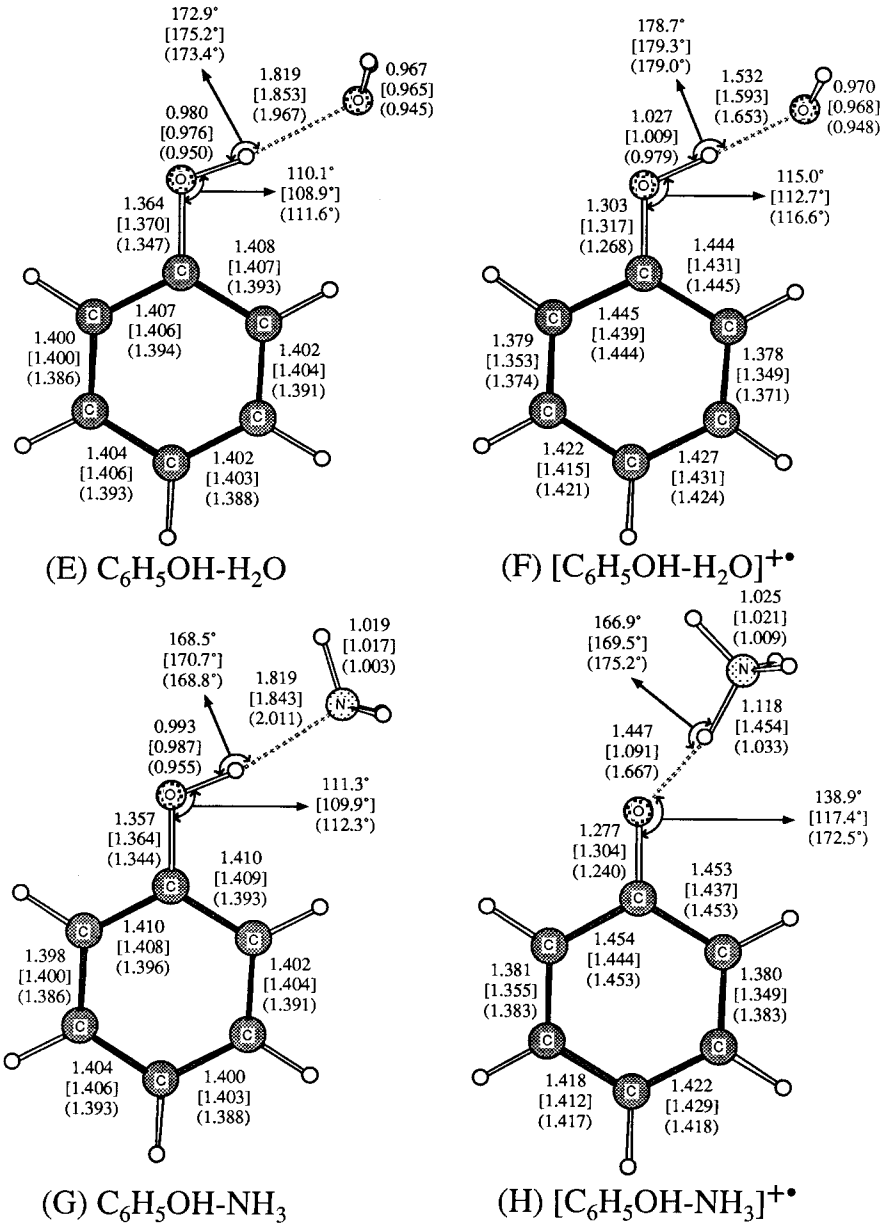

Figure 2. Optimized structures of the phenol−water (E), phenol−water cation radical (F), phenol−ammonia (G), and phenol−ammonia cation radical (H) calculated by using the B3LYP, [MP2], and (HF) methods with the DZP basis set.

complex $[C_6H_5OH-H_2O]$. Note that the hydrogen-bond length in the cation complex $[C_6H_5OH-H_2O]^{\bullet+}$ (1.532 Å) is substantially shorter than that of the neutral complex (1.819 Å) with the B3LYP method. The elongation of the O−H bond of the phenol cation radical (0.05 Å) caused by the hydrogen bond with water is also noticeable in comparison with that in the case of neutral phenol (0.01 Å). These results indicate that the ionization of phenol makes much stronger hydrogen bonds owing to the increase of acidity.

Table 3 lists the vibrational frequencies of the hydrogen-bonded complex of $[C_6H_5OH-H_2O]$ and its cation radical calculated with the B3LYP/DZP method.

In the neutral state, the O−H stretching frequency of the phenol moiety in the $[C_6H_5OH-H_2O]$ cluster is experimentally observed at 3524 cm^{-1}, resulting in a red-shift of 133 cm^{-1} from that of phenol (3657 cm^{-1}) by forming a hydrogen bond with the water molecule.[3] The corresponding value of the red-shift is evaluated to be 186 cm^{-1} with the MP2/6-31G level of calculation by Watanabe and Iwata[42] and 244 cm^{-1} with the B3LYP/DZP method.

On the other hand, the frequency shift of the O−H stretching is very remarkable in the case of the cation radical state. The O−H stretching frequency of the bare phenol cation is experimentally observed at 3535 cm^{-1},[29] and the broad spectrum is observed around the 3000 cm^{-1} region for the $[C_6H_5OH-H_2O]^{\bullet+}$ complex.[8] The corresponding frequencies obtained in the present calculation are 3732 and 2793 cm^{-1}, respectively. This large frequency shift of nearly 1000 cm^{-1} demonstrates the formation of much stronger hydrogen bonds in the ionic state than in the neutral state. Since the experimental spectrum has not been obtained in the region below 2900 cm^{-1}, we cannot definitely assign the broad band around 3000 cm^{-1} to the O−H stretching of the phenol moiety. Due to the extremely large IR intensity of the phenol O−H stretching in the $[C_6H_5OH-H_2O]^{\bullet+}$ complex, the experimentally observed broad band might be a combination band.

TABLE 3: Vibrational Frequencies of the Hydrogen-Bonded Complexes of $[C_6H_5OH-H_2O]$ and $[C_6H_5OH-NH_3]$ and Their Cation Radicals Calculated with the B3LYP/DZP Method. The Experimental Values Are Shown in Parentheses

no.	mode	$[C_6H_5OH-H_2O]$[b]	$[C_6H_5OH-H_2O]^{\bullet+}$[c]	$[C_6H_5OH-NH_3]$[d]	$[C_6H_5OH-NH_3]^{\bullet+}$
In-Plane (a′)					
1	OH str.	3601 (3524)	2793	3347 (3294)	
2	CH str.	3213 (3087)	3238	3212	3233
3	CH str.	3206 (3072)	3233	3205 (3083)	3226
4	CH str.	3194 (3054)	3226	3192 (3058)	3219
5	CH str.	3183 (3032)	3220	3181	3211
6	CH str.	3176	3215	3174	3204
7		1657	1647	1657	1609
8		1637	1539	1635	1541
9		1529	1399	1535	1413
10		1499	1475	1507	1437
11		1395	1373	1428	1368
12	CO str.	1303 (1274)	1524	1311 (1280)	1530
13		1254	1263	1281	1292
14		1358	1416	1358	1165
15		1182	1191	1180	1179
16		1169 (1151)	1163	1169	
17		1089 (1070)	1102	1088	1096
18		1037 (1026)	993	1036 (1025)	1000
19		998 (1000)	981 (977)	997 (996)	977
20		827 (825)	817 (812)	829	823
21		623 (618)	574	623	590
22		530 (528)	524 (516)	533	
23		439	475 (450)	471	495
24	acceptor molecule[a]	3826 (3650)	3801 (3625)	3624 (3333)	3561
25		1633	1652	1675	3454
26				1141	2050
27					1726
28					1530
29					1372
30	intermolecular	270 (146)	396 (328)	329 (322)	408
31		181 (151)	269 (240)	202 (164)	272
32		94	160 (≈130)	68 (60)	54
33		61	86 (84)		
Out-of-Plane (a″)					
1		997	1009	976	1004
2		961	997	958	989
3		885	942	878	929
4		835 (814)	794	818	787
5		761	805	762	806
6		702	633 (636)	701	641
7		518	454	518 (525)	470
8		419	366 (354)	418	371
9		788	1189	934 (822)	
10		225	200 (189)	228	199
11	acceptor molecule[a]	3939 (3748)	3901 (3710)	3627	3567
12				3494	3561
13				1675	1722
14					1559
15	intermolecular	256	428	287	440
16		34	70 (67)	62	56
17				33	42

[a] Acceptor molecule means H_2O or NH_3 in each complex. [b] Experimental values are taken from refs 2, 3, 5, 25, and 36. [c] Experimental values are taken from refs 8, 38, and 40. [d] Experimental values are taken from refs 12, 25, 46, and 47.

The intermolecular vibrational frequencies of the neutral and cation complexes are calculated to be 181 and 269 cm^{-1}, which correspond to the experimental values 151 and 240 cm^{-1}, respectively.[2,40] The agreement between the present theoretical values and the experimental frequencies seems to be reasonable, although intermolecular vibration is highly anharmonic.

Figure 3 summarizes the potential energy curve along the reaction coordinate with respect to the proton transfer in the $[C_6H_5OH-H_2O]^{\bullet+}$ complex. The potential energy surface involves a single energy minimum where the proton is not transferred. The stabilization energy caused by the hydrogen bonding with single water molecule shows that the cation complex is 3 times more stable than the neutral complex. The calculated charge distribution indicates that most of the positive charge (+0.885) in the $[C_6H_5OH-H_2O]^{\bullet+}$ cluster ion is located on the phenol part, as shown in Table 4. These results confirm that the proton transfer does not occur in the $[C_6H_5OH-H_2O]^{\bullet+}$ complex but the hydrogen bond between $C_6H_5OH^{\bullet+}$ and H_2O is very strong.

D. $C_6H_5OH-NH_3$ and $[C_6H_5OH-NH_3]^{\bullet+}$. Recent spectroscopic studies[1,9,10,12] concerning the proton transfer in the hydrogen-bonded cluster ion of phenol with an ammonia molecule suggest that the $[C_6H_5OH-NH_3]^{\bullet+}$ cluster ion has a double minimum potential along the proton-transfer coordinate in contrast to the case of the $[C_6H_5OH-H_2O]^{\bullet+}$ cluster. To clarify this evidence, we have calculated the geometries and the potential energy curve for the $[C_6H_5OH-NH_3]$ complex and its cation radical by using the HF, MP2, and B3LYP methods.

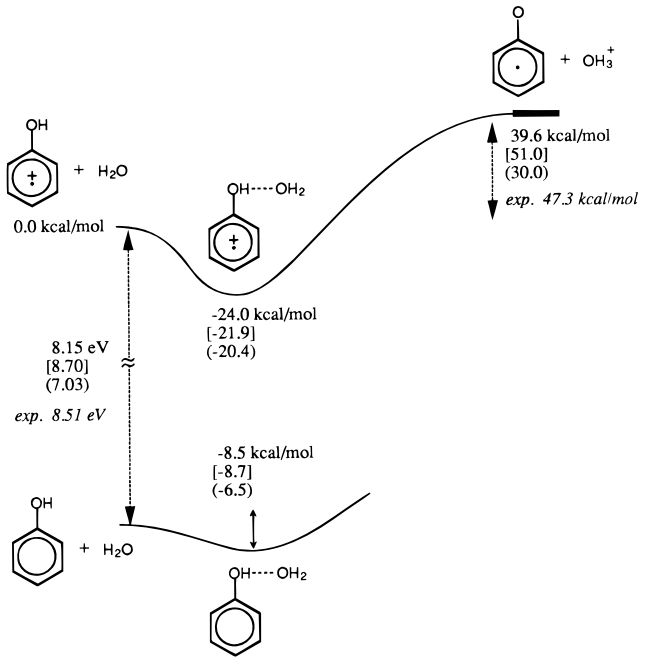

Figure 3. Potential energy curve of the $[C_6H_5OH-H_2O]$ cluster and its cation radical obtained with the B3LYP/DZP method. The values shown in the square brackets [ ] and the parentheses ( ) are calculated with the MP2/DZP and HF/DZP methods, respectively.

TABLE 4: Total Electronic Charge of Each Species in the $[C_6H_5OH-NH_3]^{\bullet+}$ and $[C_6H_5OH-(H_2O)_n]^{\bullet+}$ ($n = 1-4$) Clusters Calculated by Using the HF, MP2, and B3LYP Methods with the DZP Basis Set

compound	HF	MP2	B3LYP
$[C_6H_5OH-NH_3]^{\bullet+}$ (H)			
$C_6H_5O^{\bullet}$	0.062	0.842[a]	0.183
NH_4^+	0.938	0.158[a]	0.817
$[C_6H_5OH-H_2O]^{\bullet+}$ (F)			
$C_6H_5OH^{\bullet+}$	0.950	0.921	0.885
H_2O (a)	0.050	0.079	0.115
$[C_6H_5OH-(H_2O)_2]^{\bullet+}$ (I)			
$C_6H_5OH^{\bullet+}$	0.928	0.905	0.825
H_2O (a)	0.048	0.063	0.102
H_2O (b)	0.024	0.032	0.074
$[C_6H_5OH-(H_2O)_3]^{\bullet+}$ branched (K)			
$C_6H_5O^{\bullet}$	0.075	0.848[b]	0.200
H_3O^+ (a)	0.837	0.098[b]	0.634
H_2O (b)	0.044	0.027	0.085
H_2O (b′)	0.044	0.027	0.082
$[C_6H_5OH-(H_2O)_3]^{\bullet+}$ chained (L)			
$C_6H_5OH^{\bullet+}$	0.917	0.883	0.764
H_2O (a)	0.050	0.068	0.120
H_2O (c)	0.016	0.025	0.055
H_2O (b)	0.017	0.023	0.061
$[C_6H_5OH-(H_2O)_4]^{\bullet+}$ ringed (M)			
$C_6H_5O^{\bullet}$	0.060		0.176
H_3O^+ (a)	0.836		0.628
H_2O (c)	0.031		0.056
H_2O (c′)	0.031		0.056
H_2O (b)	0.032		0.085
$[C_6H_5OH-(H_2O)_4]^{\bullet+}$ branched (N)			
$C_6H_5O^{\bullet}$	0.034		0.113
H_2O (a)	0.039		0.073
H_3O^+ (c)	0.844		0.646
H_2O (b)	0.042		0.084
H_2O (b′)	0.042		0.083

[a] Total charges of $C_6H_5OH^{\bullet+}$ and NH_3 in the proton-nontransferred form. [b] Total charges of $C_6H_5OH^{\bullet+}$ and H_2O in the proton-nontransferred form.

The second row of Figure 2 illustrates the optimized geometries of the neutral complex $[C_6H_5OH-NH_3]$ (G) and its cation radical (H). All three methods give similar geometries for the neutral complex whose structure is the proton-nontransferred form, while a remarkable structural change is seen for the cation radical state. Note should be addressed that the optimized structures of $[C_6H_5OH-NH_3]^{\bullet+}$ are quite different depending on the methods used, although all three methods give a single energy minimum. The HF method gives an unreasonably large bond angle, $\angle C-O-H = 172.5°$, which seems to be due to the lack of electron correlation. The overestimation of the electron correlation by using the MP2 method often induces the tendency that the proton transfer hardly occurs in the hydrogen-bonded systems.

It has been already shown by the experiment that the most stable structure of the $[C_6H_5OH-NH_3]^{\bullet+}$ cluster has the proton-transferred form.[1,9,10] This evidence is consistent with the geometry obtained with the B3LYP method. The validity of the B3LYP method is also confirmed by the value of spin contamination $S^2 = 0.78$ for this system, while the values of S^2 with the HF and MP2 methods are 1.25 and 1.06, respectively.

In the case of the neutral cluster, the O−H bond length of the phenol moiety (0.993 Å) is slightly larger than that of the $[C_6H_5OH-H_2O]$ complex (0.980 Å), since the calculated proton affinity (PA) of the NH_3 molecule (207 kcal/mol) is larger than the PA of the H_2O molecule (168 kcal/mol) with the B3LYP method. The experimental values of PA are 208 kcal/mol for NH_3 and 165 kcal/mol for H_2O.[43−45]

As a result of optimization with the B3LYP method in the case of the cationic state, the $[C_6H_5OH-NH_3]^{\bullet+}$ cluster ion turns out to be the hydrogen-bonded complex between the NH_4^+ ion and phenoxy π radical, since the hydrogen atom of the phenol cation radical is strongly attached to the NH_3 molecule.

Table 3 lists the calculated vibrational frequencies of the $[C_6H_5OH-NH_3]$ cluster and its cation radical together with those of the neutral $[C_6H_5OH-H_2O]$ complex and its cation radical. The results obtained with the present calculation agree well with the experimental[2,3,5,8,12,25,36,38,40,46,47] and other theoretical values.[37,39,41] The OH stretching frequency of the neutral $[C_6H_5OH-NH_3]$ complex (3347 cm^{-1}) is red-shifted by 254 cm^{-1} compared to that of the neutral complex $[C_6H_5OH-H_2O]$ (3601 cm^{-1}) owing to the increasing value of the PA in the acceptor molecule. There is no vibrational frequency corresponding to the OH stretching mode of phenol in the $[C_6H_5O^{\bullet}-NH_4^+]$ complex because the proton is completely transferred. The intermolecular vibrational frequency of the neutral $[C_6H_5OH-NH_3]$ complex is experimentally observed[12] at 164 cm^{-1}, which well corresponds to the calculated frequency 202 cm^{-1} with the B3LYP method.

The charge distribution calculated with the B3LYP method shown in Table 4 clearly indicates that most of the positive charge (+0.817) is located on the NH_4^+ moiety.

Figure 4 summarizes the potential energy curve of the proton transfer for the $[C_6H_5OH-NH_3]$ complex and its cation radical. In this system, it is also found that the stabilization energy by the hydrogen bonding of the cationic state is 3 times larger than that of the neutral state.

The difference of the PAs between H_2O and NH_3 causes the stronger hydrogen bonding for the $[C_6H_5OH-NH_3]$ cluster than for the $[C_6H_5OH-H_2O]$ cluster. The stabilization energy of the $[C_6H_5O^{\bullet}-NH_4^+]$ complex relative to the energy of $C_6H_5OH^{\bullet+} + NH_3$ is evaluated to be 33.2 kcal/mol, which is 9.2 kcal/mol larger than that in the case of the $[C_6H_5OH-H_2O]^{\bullet+}$ complex (24.0 kcal/mol). As suggested by the experiment,[1,10] two dissociation limits, $C_6H_5OH^{\bullet+} + NH_3$ and $C_6H_5O^{\bullet} + NH_4^+$, lie in almost the same energy. This evidence agrees with

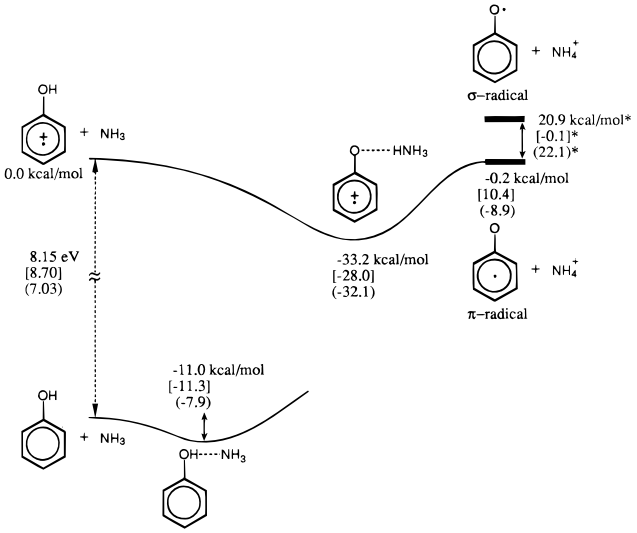

Figure 4. Potential energy curve of the $[C_6H_5OH-NH_3]$ cluster and its cation radical obtained with the B3LYP/DZP method. The values shown in the square brackets [ ] and the parentheses ( ) are calculated with the MP2/DZP and HF/DZP methods, respectively. The values indicated with * are the energy difference between phenoxy π- and σ-radicals.

the result that the calculated energy difference of the two dissociation limits is only 0.2 kcal/mol with the B3LYP method. On the other hand, the dissociation limit $C_6H_5O^{\bullet} + H_3O^+$ is 47.3 kcal/mol higher than that of $C_6H_5OH^{\bullet+} + H_2O$, and this energy difference is calculated to be 39.6 kcal/mol with the B3LYP method.

Recent experimental studies[1,10] suggest that the $[C_6H_5OH-NH_3]^{\bullet+}$ complex has a double-well potential surface along the proton-transfer coordinate. Steadman and Syage indicated that there is substantial energy barrier (ca. 1 eV) along the reaction coordinate from inner potential well to dissociative proton transfer in this system.[10]

It is noted that our present study indicates the single potential well along the reaction coordinate for proton transfer in the $[C_6H_5OH-NH_3]^{\bullet+}$ cluster ion whose energy minimum corresponds to the proton-transferred structure. We could not find any other energy minimum corresponding to the proton-nontransferred structure. This result is consistent with the recent ab initio study by Bertrán et al. on this system obtained at their highest level of calculation.[41] The discrepancy between theoretical potential energy surface and experimentally suggested double-well potential must be argued in a future study.

E. $[C_6H_5OH-(H_2O)_n]^{\bullet+}$ ($n \geq 2$) Clusters. The experimental and theoretical studies for the neutral hydrogen-bonded clusters $[C_6H_5OH-(H_2O)_n]$ ($n = 1-4$) show the fact that proton transfer does not occur in this neutral system,[3−5,42,48,49] where the most stable structures are hydrogen-bonded complexes between the phenol and the ringed water clusters $(H_2O)_n$.[42]

On the other hand, recent experiments[1,7,8] with the ion-trapping technique for the $[C_6H_5OH-(H_2O)_n]^{\bullet+}$ ($n = 1-4$) clusters demonstrate that the proton transfer occurs in the $n \geq 3$ clusters, but not in the $n = 1$ and $n = 2$ clusters. Their analysis of the IR spectra suggests that the proton-transferred complex does not have a hydrogen-bonded ringed structure shown in the neutral cluster but has a branched structure involving an H_3O^+ ion.[8] To examine these experimental suggestions, we have calculated the stable structures and their vibrational frequencies for these ion clusters. We will mainly discuss with the results obtained by the B3LYP method for the reason mentioned in the previous section III-A and B.

1. $n = 2$ Cluster. Figure 5 illustrates the optimized structures of the $n = 2$ cluster, $[C_6H_5OH-(H_2O)_2]^{\bullet+}$ (I), and the water dimer (J) calculated by using the HF, MP2, and B3LYP methods with the DZP basis set. All three methods give similar structures for this cluster. There is no significant structural change in the phenol cation radical moiety compared to the $n = 1$ cluster ion and the most of positive charge (+0.825) is located on the phenol part. The present result indicates that hydrogen-bonded complex between $C_6H_5OH^{\bullet+}$ and $(H_2O)_n$ is formed at the $n = 2$ cluster without conversion to the $[C_6H_5O^{\bullet}-H^+(H_2O)_2]$ complex.

We have also confirmed that the cyclic structure[42] obtained in the case of the neutral cluster $[C_6H_5OH-(H_2O)_2]$ is not the energy minimum for the cationic state and is optimized to the structure (I) shown in Figure 5. The ability of the oxygen atom of phenol as a proton acceptor is smaller in the phenol cation radical than in neutral phenol, because the hybridization of the oxygen atom of the phenol cation radical is more like sp^2 rather than sp^3, which is that of neutral phenol. This increasing σ character of the oxygen atom in the cation radical leads to the chained structure being more favorable than the cyclic form. The chained structure is also suggested in the case of $(phenol)_n^+$ clusters.[50]

Although the proton transfer does not occur in the $n = 2$ cluster size, the O−H bond length of the phenol moiety (1.074 Å) becomes 0.047 Å longer and the hydrogen-bond length between $C_6H_5OH^{\bullet+}$ and $(H_2O)_2$ (1.393 Å) becomes 0.139 Å shorter compared to those of the $[C_6H_5OH-H_2O]^{\bullet+}$ cluster. Moreover, the hydrogen-bond length between two H_2O molecules in the $[C_6H_5OH-(H_2O)_2]^{\bullet+}$ cluster is found to be 0.27 Å shorter than that in the water dimer (1.897 Å), as shown in Figure 5. The PA of the water dimer is calculated to be 203 kcal/mol with the B3LYP method, which is much larger than that of the water monomer (168 kcal/mol). These results clearly demonstrate that the hydrogen bond becomes stronger as the PA of the acceptor molecule increases.

2. $n = 3$ Cluster. Figure 6 shows the optimized structures of the most probable two isomers for the $[C_6H_5OH-(H_2O)_3]^{\bullet+}$ clusters, whose structures have branched (K) and chained (L) forms for hydrogen bonding. The relative energies of the two isomers are summarized in Table 5. Since the obtained geometries vary depending on the methods used, we will first discuss the results of the B3LYP method and consider the difference among the methods later.

The optimized structures calculated with the B3LYP method show that the branched structure (K) has the proton transferred form and the chained structure (L) has the proton-nontransferred form. The former is 1.8 kcal/mol more stable than the latter. In the case of branched isomer (K), the large stabilization caused by the proton transfer can be rationalized by the fact that the positive charge on the H_3O^+ moiety well disperses through the three hydrogen bonds toward the phenoxy radical and two water molecules. The calculated charge distribution shows that most of the positive charge (+0.634) is located on the H_3O^+ ion and that the remaining positive charge spreads to the surrounding molecules, as listed in Table 4. In the case of the chained structure (L), the hydrogen-bond distance between the phenol cation radical and the water trimer is extremely short (1.286 Å), although proton transfer does not occur. The calculated charge distribution of the chained form (L) indicates that the positive charge on the phenol ring oozes out to the water molecules. The present result obtained with the B3LYP method demonstrates that the branched structure, being the proton

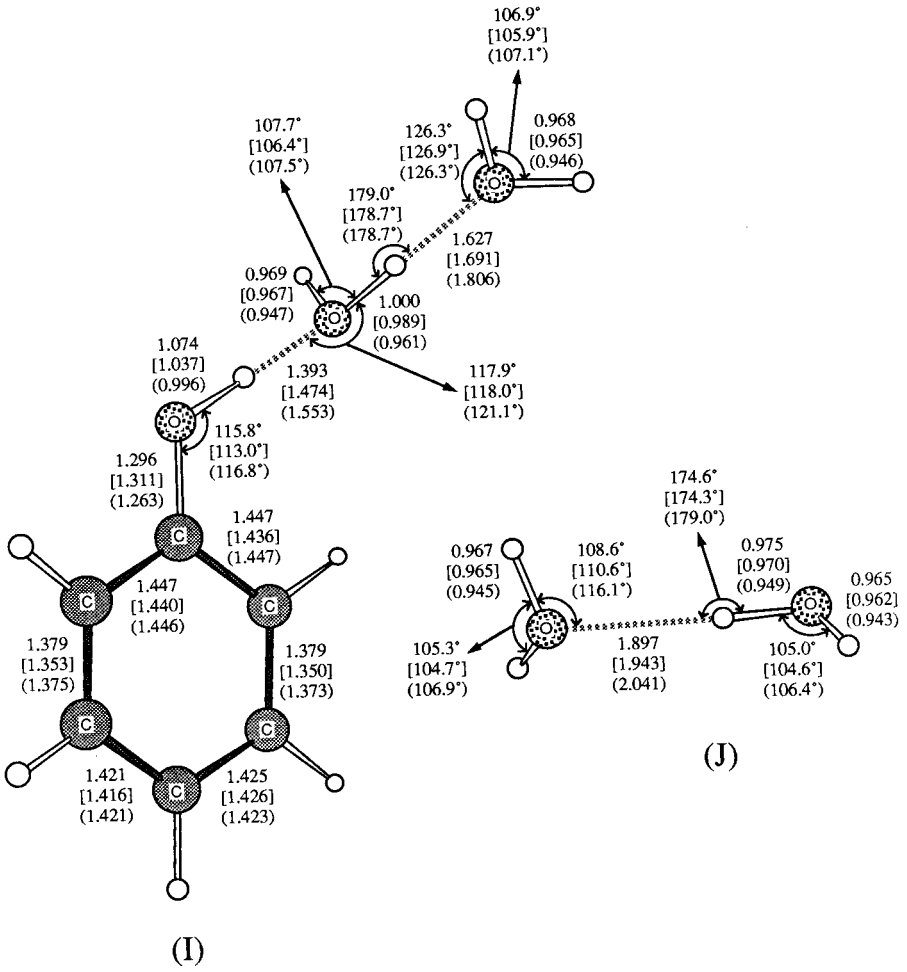

Figure 5. Stable structures of the $[C_6H_5OH-(H_2O)_2]^{\bullet+}$ cluster (I) and the water dimer (J) calculated by using the B3LYP, [MP2], and (HF) methods with the DZP basis set.

transferred form, is more favorable than the chained structure, being the proton-nontransferred form, in the $n = 3$ size cluster.

In the case of the $n = 3$ clusters, the calculated results with the HF and MP2 methods differ from the above results. In the HF calculation, the proton-transferred and -nontransferred structures are located at the energy minimum for both branched and chained isomers. The proton-transferred form is the most stable in the branched structure, and the nontransferred form in the chained structure is the most stable. Although both potential surfaces for the two isomers show a double minimum along the proton-transfer coordinate, the energy barriers from the less stable isomers are extremely small (less than 1.0 kcal/mol). Moreover, the energy minima of the less stable isomers disappear when we corrected the zero-point vibrational energies in the HF calculation. Consequently, the result obtained with the HF method is similar to the result with the B3LYP method for the potential energy surface as well as the stable structures.

On the other hand, the optimized structures for the two isomers with the MP2 method are both the proton-nontransferred form. The stability between the two isomers is, however, consistent with the result obtained with the B3LYP method.

Considering the tendency of the proton transfer obtained with the MP2 method, we can conclude that most of the hydrogen-bonded cluster at the size $n = 3$ exists as the branched $[C_6H_5O^{\bullet}-H^+(H_2O)_3]$ form.

3. $n = 4$ Cluster. We have carried out the calculation for the $n = 4$ cluster, $[C_6H_5OH\ (H_2O)_4]^{\bullet+}$, by using the HF and B3LYP methods, since the geometry optimization with the MP2 method is very time-consuming for large clusters. In the case of $n = 4$ cluster ions, there are two distinctive isomers, namely, the ringed structure (M) and the branched structure (N), as illustrated in Figure 7.

The obtained structures with the B3LYP method indicate that both isomers are the proton-transferred form and there is no local minimum for the proton-nontransferred structure. The ringed structure (M) is calculated to be 2.5 kcal/mol more stable than the branched structure (N). There is a structural similarity between the two isomers of the $n = 4$ cluster ion and the branched form of the $n = 3$ cluster ion, $[C_6H_5O^{\bullet}-H^+(H_2O)_3]$, where the positive charge on the H_3O^+ ion is fully stabilized through the three hydrogen bonds. The detailed charge distributions are listed in Table 4.

The HF method gives results similar to the B3LYP method except for the case of the ringed isomer, which has a very shallow energy minimum for the proton-nontransferred structure, but this energy minimum disappears by the correction of zero-point vibrational energies.

As a result of the correction of zero-point vibrational energies with the B3LYP method, the energy difference between the ringed structure and the branched isomer in the $n = 4$ cluster size becomes ca. 1 kcal/mol. Consequently, we can conclude that the two isomers of $[C_6H_5OH-(H_2O)_4]^{\bullet+}$ have the proton-transferred form, $[C_6H_5O^{\bullet}-H^+(H_2O)_4]$, and both ringed and branched structures would coexist.

F. Potential Energy Surfaces of $n = 1-4$ Cluster Ions. Figure 8 summarizes the potential energy surfaces obtained with the B3LYP method for the hydrogen-bonded cluster ions $[C_6H_5OH-(H_2O)_n]^{\bullet+}$ ($n = 1-4$). Table 5 lists the total energies

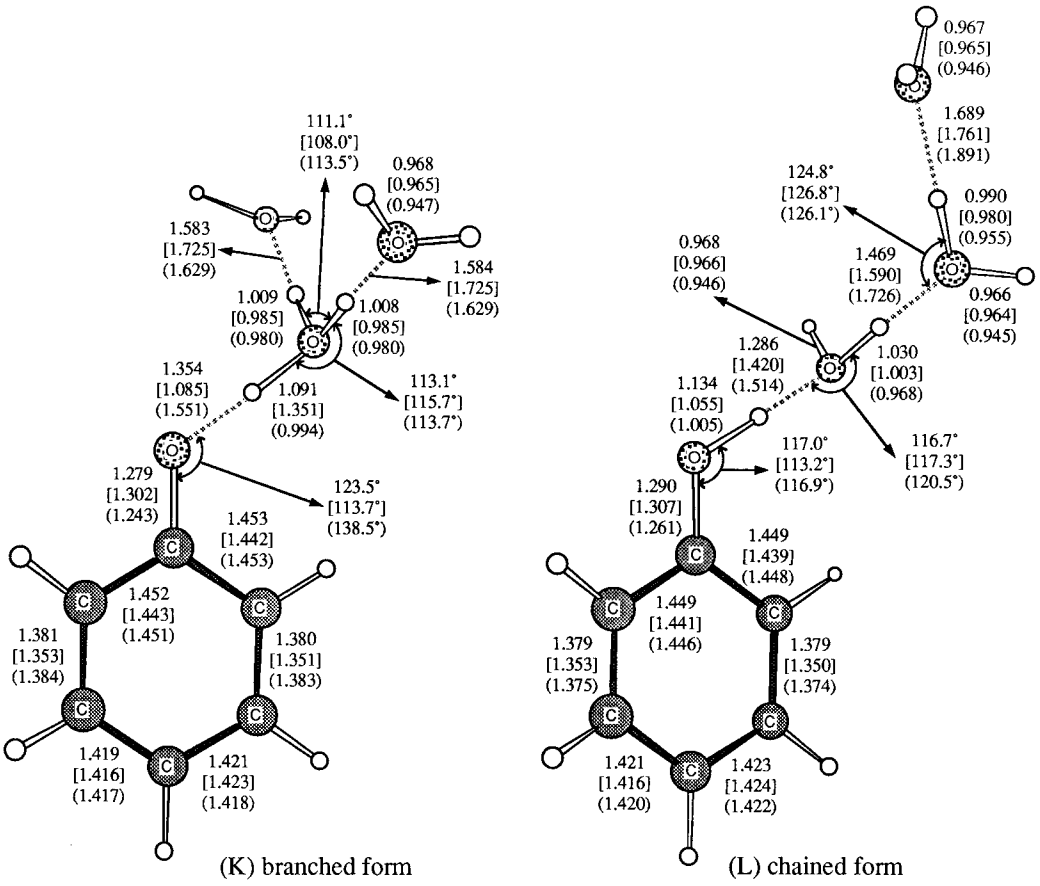

Figure 6. Optimized structures of the branched (K) and chained (L) forms of the $[C_6H_5OH-(H_2O)_3]^{\bullet+}$ cluster calculated by using the B3LYP, [MP2], and (HF) methods with the DZP basis set.

TABLE 5: Total Energies (*E* (hartree)), Relative Energies (ΔE (kcal/mol)), and Relative Energies Corrected with Zero-Point Vibrations (ΔE_{zpvc} (kcal/mol)) for the $[C_6H_5OH-(H_2O)_n]^{\bullet+}$ Cluster Ions Calculated by Using the HF, MP2, and B3LYP Methods with the DZP Basis Set

	HF method			MP2 method			B3LYP method		
	E (hartree)	ΔE (kcal/mol)	ΔE_{zpvc} (kcal/mol)	*E* (hartree)	ΔE (kcal/mol)	ΔE_{zpvc} (kcal/mol)	*E* (hartree)	ΔE (kcal/mol)	ΔE_{zpvc} (kcal/mol)
(A) C_6H_5OH	−305.623 20	0.0	0.0	−306.574 27	0.0	0.0	−307.519 12	0.0	0.0
(B) $C_6H_5OH^{\bullet+}$	−305.364 99	7.03 eV	7.00 eV	−306.254 61	8.70 eV	8.76 eV	−307.219 72	8.15 eV	8.15 eV
(D) $C_6H_5O^{\bullet}$ (π)	−305.032 64	0.0	0.0	−305.892 52	0.0	0.0	−306.875 44	0.0	0.0
(C) $C_6H_5O^{\bullet}$ (σ)	−304.997 49	0.96 eV	0.98 eV	−305.892 75	−0.01 eV	−0.05 eV	−306.842 19	0.90 eV	0.90 eV
(H) $C_6H_5OH-NH_3^{\bullet+}$	−361.625 79			−362.695 20			−363.843 79		
(F) $C_6H_5OH-H_2O^{\bullet+}$	−381.444 44			−382.532 35			−383.703 09		
(I) $C_6H_5OH-(H_2O)_2^{\bullet+}$	−457.512 39			−458.799 91			−460.175 69		
$C_6H_5OH-(H_2O)_3^{\bullet+}$									
(K) branched transf.	−533.581 21	0.0	0.0				−536.646 30	0.0	0.0
branched TS	−533.576 46	3.0	0.5				NA		
branched nontransf.	−533.577 55	2.3	2.4	−535.064 40	0.0		NA		
chained transf.	−533.573 07	5.1	4.7	NA			NA		
chained TS	−533.571 52	6.1	3.7	NA			NA		
(L) chained nontransf.	−533.575 66	3.5	4.2	−535.062 96	0.9		−536.643 49	1.8	1.6
$C_6H_5OH-(H_2O)_4^{\bullet+}$									
(M) ringed transf.	−609.647 51	0.0	0.0				−613.116 64	0.0	0.0
ringed TS	−609.640 80	4.2	1.9				NA		
ringed nontransf.	−609.641 08	4.0	3.7				NA		
(N) branched transf.	−609.646 23	0.8	−0.4				−613.112 69	2.5	1.1

and the relative energies with and without correction of the zero-point vibrational energies calculated with three different methods.

The potential curves have a single energy minimum for each size of cluster ions with the B3LYP method. It is found by these energy curves that the $n = 3$ (branched) and $n = 4$ clusters have the proton-transferred form $[C_6H_5O^{\bullet}-H^+(H_2O)_n]$ ($n = 3$, 4), while the $n = 1$, 2 and $n = 3$ (chained) cluster ions have the proton-nontransferred form $[C_6H_5OH^{\bullet+}-(H_2O)_n]$ ($n = 1-3$).

Table 6 shows that the stabilization energy by hydrogen bonding becomes large as the number of acceptor molecules increases. As described in the previous sections, it is clear that the value of PA becomes large as the number of acceptor molecules increases. Namely, the $[C_6H_5OH^{\bullet+}-(H_2O)_n]$ cluster ions undergo larger stabilization by hydrogen bonding with more water molecules, which leads to the proton-transferred structure, $[C_6H_5O^{\bullet}-H^+(H_2O)_n]$, at the $n = 3$ (branched) cluster ion. The MP2 calculation also gives the result that the stabilization

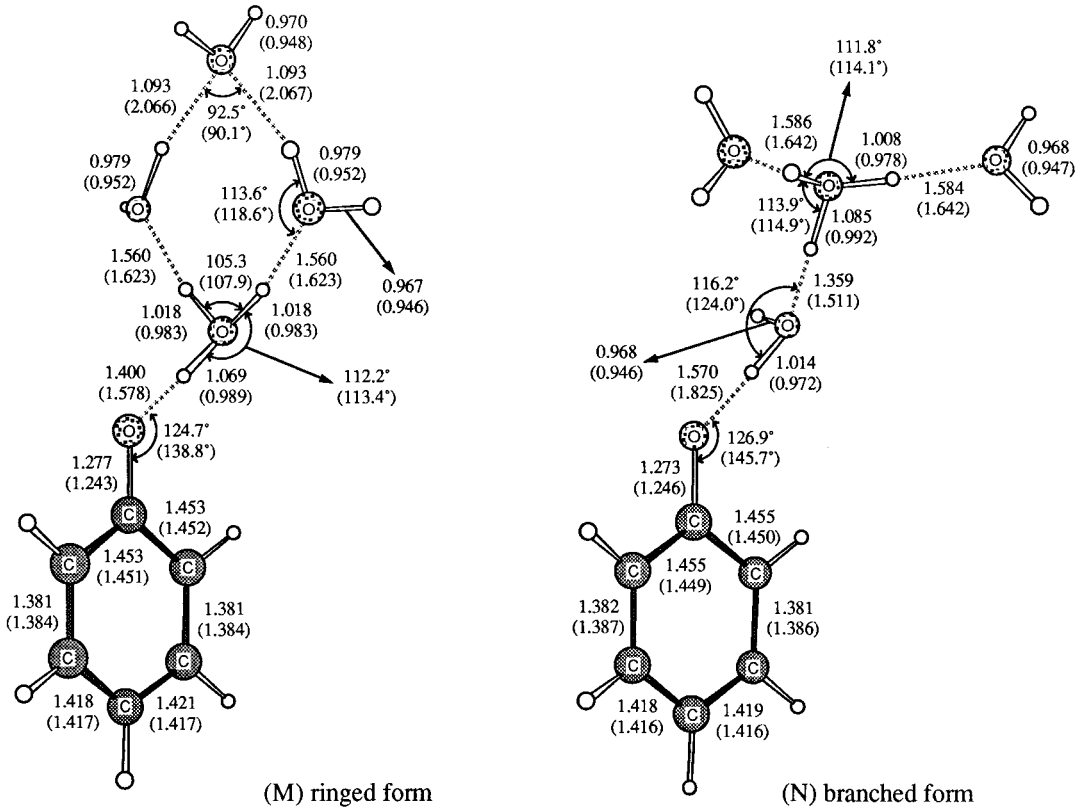

Figure 7. Optimized geometries of the ringed (M) and branched (N) isomers of the $[C_6H_5OH-(H_2O)_4]^{\bullet+}$ cluster calculated by using the B3LYP and (HF) methods with the DZP basis set.

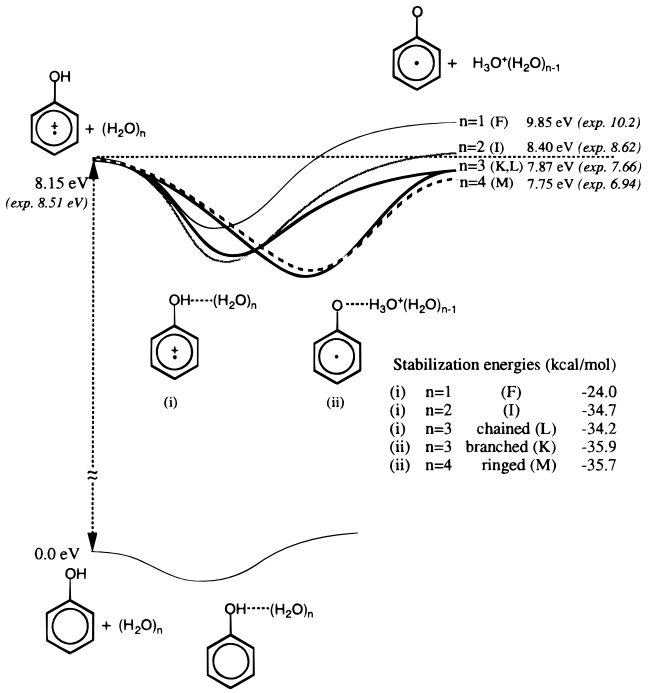

Figure 8. Potential energy curves of the $[C_6H_5OH-(H_2O)_n]^{\bullet+}$ (n = 1−4) clusters obtained by using the B3LYP/DZP method. The experimental values shown in parentheses are taken from refs 38, 44, 45, and 51.

energies by hydrogen bonding become large as the number of acceptor molecules increases, although the MP2 method gives only the proton nontransferred forms for the $n = 1-3$ cluster ions.

The experimental values of the dissociation energies to the proton-transferred species, $C_6H_5O^{\bullet} + H^+(H_2O)_n$, relative to the neutral state, $C_6H_5OH + (H_2O)_n$, are 10.2, 8.62, 7.66, and 6.94 eV for $n = 1-4$, respectively.[44,45,51] These values have good correspondence with the calculated values with the B3LYP method, as shown in Figure 8.

Although the HF method indicates that the potential energy surfaces for the $n = 3$ and $n = 4$ cluster ions have double-well structure, the single-well potentials for both clusters seem to be appropriate, since the small energy barriers vanish after the correction of zero-point vibration, as shown in Table 6. This result also supports the validity of the potential energy surfaces calculated with the B3LYP method shown in Figure 8.

G. IR Spectra for $n = 1-4$ Cluster Ions. Figure 9 depicts the calculated IR spectra for the $[C_6H_5OH-(H_2O)_n]^{\bullet+}$ ($n = 1-4$) cluster ions obtained by using the B3LYP method. In all spectra, relatively strong peaks derived from the C−H bending of the phenyl ring and the O−H bending frequencies (ν_2) of the water molecules appear around the 1200−1500 cm^{-1} region. Although these two types of bands are assigned to C−H bending and the O−H bending in Figure 9, some of these bands are strongly coupled to each other. The in-plane and out-of-plane bending frequencies of the phenol O−H are also seen in the same region of the spectra for the proton-nontransferred structures (F), (I), and (L) with strong intensity for the former and relatively weak intensity for the latter. On the other hand, the bands that are due to the H_3O^+ ion appear in the 1000−1700 cm^{-1} region of the spectra for the proton-transferred forms (K), (M), and (N). The peaks below 1000 cm^{-1} are mainly attributed to the vibrational modes of the phenyl ring moiety (mostly the 500−1000 cm^{-1} region) and the water moieties (below the 600 cm^{-1} region). The C−H stretches of the phenyl ring do not appear in all spectra because of the very weak intensity as reported in the experimental study,[3] although the corresponding peaks are calculated to be around the 3200 cm^{-1} region and these frequencies do not depend on the cluster size.

TABLE 6: Stabilization Energies without (ΔE) and with (ΔE_{zpvc}) the Zero-Point Vibrational Correction of the $[C_6H_5OH-(H_2O)_n]^{\bullet+}$ ($n = 1-4$) Cluster Ions Relative to the Phenol Cation Radical and Water Clusters $(H_2O)_n$ Calculated by Using the HF, MP2, and B3LYP Methods with the DZP Basis Set

	HF method		MP2 method		B3LYP method	
	ΔE (kcal/mol)	ΔE_{zpvc} (kcal/mol)	ΔE (kcal/mol)	ΔE_{zpvc} (kcal/mol)	ΔE (kcal/mol)	ΔE_{zpvc} (kcal/mol)
$C_6H_5OH^{\bullet+} + (H_2O)_n \rightarrow [C_6H_5OH-(H_2O)_n]^{\bullet+}$						
$n = 1$ (F)	20.4	18.4	21.9	19.6	24.0	22.2
$n = 2$ (I)	28.6	26.8	31.1		34.7	33.7
$n = 3$						
(L) chained (nontransferred)	29.0	28.6	30.4		34.2	35.9
chained (transferred)	27.3	28.1				
branched (nontransferred)	30.2	30.5	31.3			
(K) branched (transferred)	32.4	32.8			35.9	37.5
$n = 4$						
ringed (nontransferred)	29.4	30.2				
(M) ringed (transferred	33.4	33.9			35.7	36.4
(N) branched (transferred)	32.6	34.3			33.2	35.4

We will focus on the O−H stretching frequencies in order to provide direct evidence of proton transfer in the following discussions. In the spectra shown in Figure 9, the scaling is not carried out for all vibrational frequencies, since our interest lies in the comparison of the calculated spectral patterns with the experimentally observed ones.

1. O−H Stretching Frequency of the Phenol Moiety. It is well-known that the O−H stretching frequency of the proton-donating moiety in the hydrogen-bonded system shows substantial red-shift from the free O−H stretching frequency. In the IR spectrum of the $n = 1$ cluster ion $[C_6H_5OH-H_2O]^{\bullet+}$, the O−H stretching frequency of the phenol moiety appears at 2793 cm^{-1}, which is 939 cm^{-1} red-shifted by hydrogen bonding compared to that of the bare phenol cation radical (3732 cm^{-1}). Recently, Fujii et al. reported the significant red-shift (475 cm^{-1}) of the O−H stretching frequency of the phenol ion in the π-type hydrogen-bonded complex with benzene.[50] The evaluated value of the red-shift, 939 cm^{-1}, is much larger than that of the [phenol−benzene]$^+$ cluster ion, since the $[C_6H_5OH-H_2O]^{\bullet+}$ cluster ion contains the σ-type hydrogen bonding between the phenol cation radical and the water molecule. The O−H stretching band of the $n = 2$ cluster ion has lower frequency (2076 cm^{-1}) than that of the $n = 1$ cluster ion because of the increasing basicity of the acceptor moiety, and the red-shift from that of the $n = 1$ cluster ion by the hydrogen bonding is evaluated to be 717 cm^{-1}. The calculated O−H stretching frequency of the $n = 3$ cluster ion (L) appears at 1253 cm^{-1}, resulting in the red-shift by 823 cm^{-1} compared to that of the $n = 2$ cluster ion. It is outstanding that the O−H stretching frequency of the phenol cation radical exhibits the remarkable red-shift by 700−900 cm^{-1} as the number of water molecules increases one by one. In the cases of the $n = 3$ branched form (K) and $n = 4$ cluster ions, there is no band corresponding to the O−H stretching of the phenol moiety, since proton transfer is completed in these cluster ions.

The experimental spectra indicate the increase of intensity and the broadning of the phenol O−H stretching.[3,25,47] Our calculation shows that the infrared absorption intensity of the O−H stretching of the phenol cation radical (266.0 km/mol) is extremely enhanced by 11.7 and 18.4 times owing to the hydrogen bonding with a single water molecule and two water molecules, respectively. The large intensity is also obtained for the phenoxy O···H stretching in the proton-transferred structures, (K), (M), and (N). These intermolecular vibrations belong to the asymmetric stretching of the proton between two oxygens, O···H−O, whose frequencies are calculated to be 1896, 2109, and 2987 cm^{-1} for the structures (K), (M), and (N), respectively. The tendency of these frequencies well corresponds to the O−H bond distances of H_3O^+ but not the intermolecular distances between phenoxy O···H.

2. O−H Stretching Frequencies of the Water Molecules. We will discuss the calculated IR spectra for the $[C_6H_5OH-(H_2O)_n]^{\bullet+}$ ($n = 1-4$) clusters by comparing with the experimentally observed one.[8]

The symmetric and asymmetric O−H stretching frequencies of water molecule in the $n = 1$ cluster ion are calculated to be 3801 and 3901 cm^{-1}, respectively. These values are close to those of the neutral water molecule, which are calculated to be 3831 and 3951 cm^{-1}, respectively. These calculated values 3801, 3901, 3831, and 3951 cm^{-1} agree well with the corresponding experimental values, 3625, 3710, 3657, and 3756 cm^{-1}, if they are scaled by 1.05. The IR intensity of the water moiety in the spectrum for the $n = 1$ cluster ion (160.1 km/mol for ν_3 and 80.1 km/mol for ν_1) is shown to be strongly enhanced by forming the hydrogen bond compared to those of the bare water molecule (34.3 km/mol for ν_3 and 3.9 km/mol for ν_1) with the B3LYP method. Similar intensity enhancement of the O−H stretches of water molecules is observed by Choi et al. in the $[NO^+-(H_2O)_n]$ cluster ions using infrared multiphoton dissociation spectroscopy.[52]

In the spectra of $n \geq 2$ cluster ions, it is found that the O−H stretching frequencies of the terminal water molecule (b or b′) located at the outermost side of the hydrogen-bond chain always appear at the 3800−3900 cm^{-1} region without significant red-shift. On the other hand, there are two types of O−H stretches in the water molecules (a and c) which take part in the hydrogen-bonded chain or ring at the inside. One of the O−H bonds of each water molecule is participating in the hydrogen bonding and the other is a free O−H bond without hydrogen bonding. In the cases of $n = 2$ and $n = 3$ (chained) cluster ions, the stretching frequencies of the hydrogen-bonded O−H bonds exhibit a large red-shift, while those of the free O−H bonds stay at the 3800−3900 cm^{-1} region.

The calculated spectral pattern of the O−H stretches for the $n = 2$ cluster ion indicates two strong bands at 3870 and 3937 cm^{-1} and a weak band at 3830 cm^{-1}. These three O−H stretching frequencies of two water molecules seem to be consistent with the experimentally observed bands, an intense band at 3685 cm^{-1}, a shoulder around 3730 cm^{-1}, and a weak band at 3640 cm^{-1}, respectively.[8] A very broad band observed around 3200 cm^{-1} would be assigned to the extremely strong peak of the hydrogen-bonded O−H stretching of the intermediate water molecule (a) calculated at 3261 cm^{-1}.

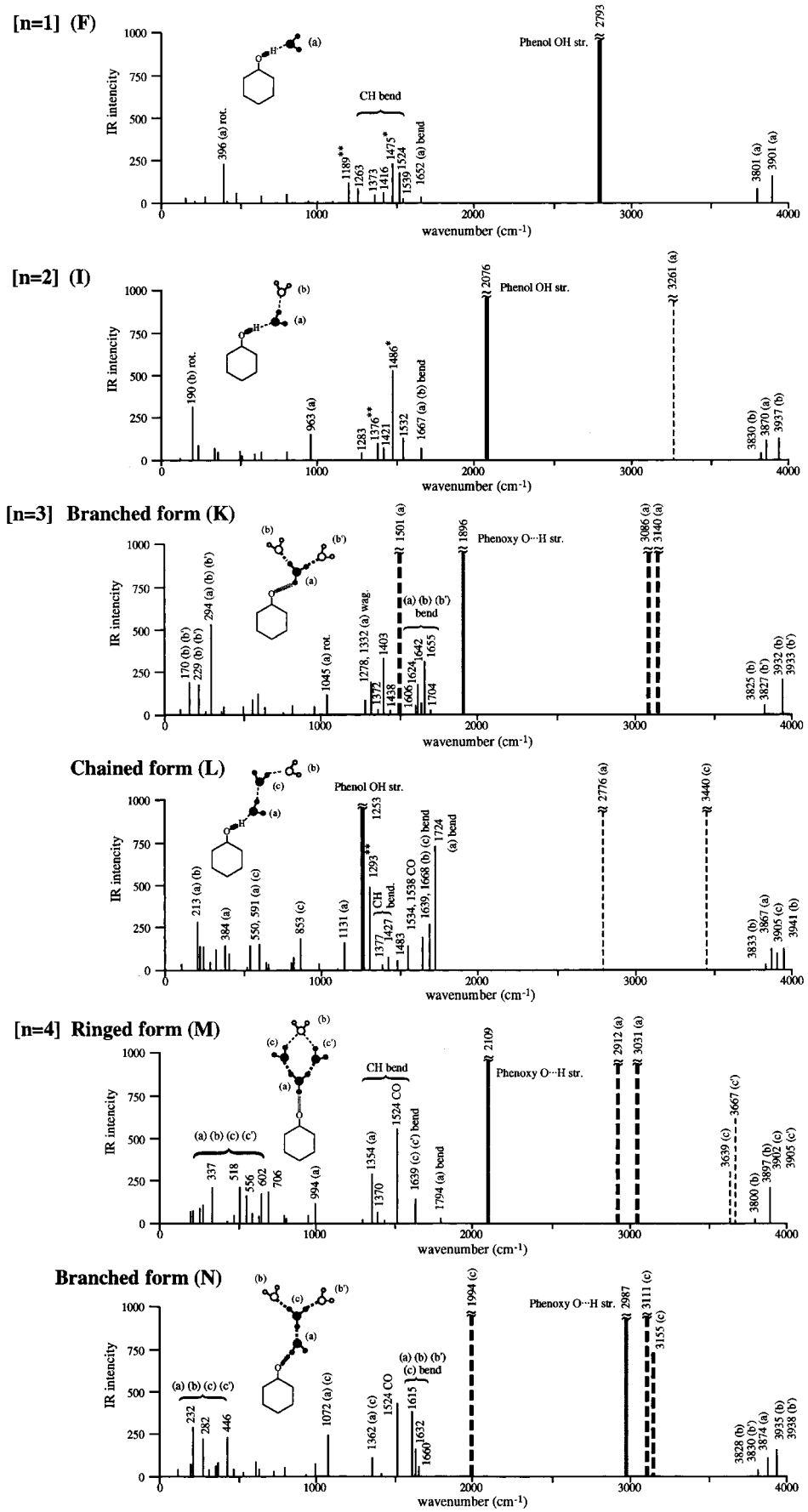

Figure 9. The calculated IR spectra of the $[C_6H_5OH-(H_2O)_n]^{\bullet+}$ ($n = 1-4$) clusters obtained with the B3LYP/DZP method. In all spectra, bold lines, bold dotted lines, and dotted lines designate the phenol O−H or phenoxy O···H stretching, the hydrogen-bonded O−H stretching of the H_3O^+ moiety, and the hydrogen-bonded O−H stretching of the water molecules, respectively. The peaks indicated with * and ** correspond to the in-plane and out-of-plane bending modes of the phenol O−H, respectively.

As shown in the spectrum of the chained structure (L) of the $n = 3$ cluster ion, the O−H stretching frequency of the water molecule (a) adjacent to the phenol cation radical is calculated to be 2776 cm^{-1}, whose red-shift is extremely large compared to the frequency 3440 cm^{-1} of the median water molecule (c). There are four peaks of the free O−H stretching of the water molecules. On the other hand, we have obtained two intense O−H bands at 3825 and 3932 cm^{-1} in the spectrum of the branched structure (K) of the $n = 3$ cluster ion, which is the proton-transferred form. These two peaks agree well with the experimentally observed ones, 3637 and 3730 cm^{-1}.[8] Moreover, the extremely broad band observed around 3100 cm^{-1} may be attributed to the two peaks of the O−H stretching of the H_3O^+ ion calculated at 3086 and 3140 cm^{-1}.

The calculated spectra for the ringed (M) and branched (N) forms of the $n = 4$ cluster ions resemble the spectrum of the branched structure (K) of the $n = 3$ cluster ion owing to the structural similarity. Among the three species (K), (M), and (N), the strong bands in the 1900−2100 cm^{-1} region are mainly due to the O−H stretching of the H_3O^+ connecting to the phenoxy moiety, although the peaks for (K) and (M) are assigned to the phenoxy O···H streching in Figure 9. The hydrogen-bonded O−H stretching of the H_3O^+ toward the H_2O molecules varies from 2900 to 3150 cm^{-1} depending on the strength of their hydrogen bonds.

In the case of the ringed form (M), there are two peaks of the free O−H stretching over the 3800 cm^{-1} region, whereas three peaks appear for the branched isomer (N). The IR spectrum observed for the $n \geq 4$ cluster ions in the 2900−3800 cm^{-1} region seems to correspond well to the calculated spectrum of the ringed form (M) of the $n = 4$ cluster ion, although the experimental spectrum is not highly resolved. Although a broad and intense band whose peak is 3370 cm^{-1} has not been characterized yet, this band seems to correspond to the hydrogen-bonded O−H stretching of the median waters (c and c′) calculated at 3639 and 3667 cm^{-1}.

From these results, we have found that the theoretically predicted spectra for $n = 1-4$ clusters, which correspond to the most stable structures among isomers, show reasonable agreement with the experimental IR spectra.[8] In the case of $n = 3$ cluster ions, the calculated IR spectrum of the proton-transferred branched form (K) has good correspondence with the reported IR spectrum. Considering the small energy difference between the two isomers of the $n = 3$ cluster ions (K) and (L), the proton-nontransferred isomer (L) can also contribute to the experimentally observed spectrum. Since the energy difference between branched (N) and ringed (M) structures of the $n = 4$ cluster ions is also small, the experimentally observed IR spectrum is expected to be a mixture of the spectra of the two isomers (N) and (M).

IV. Conclusion

The hydrogen-bonded cluster ions of phenol with water molecules $[C_6H_5OH-(H_2O)_n]^{\bullet+}$ ($n = 1-4$) exhibit quite different properties on the proton transfer in comparison with that of the neutral state. In contrast to the neutral clusters, proton transfer occurs easily in the ion clusters because of the increasing acidity of the phenol molecule due to the ionization. Moreover, the increase of the number of H_2O molecules induces large stabilization by the hydrogen bonding and results in the proton transfer at the $n \geq 3$ cluster ions.

The present computational study clearly confirms that the proton transfer in the hydrogen-bonded cluster ions $[C_6H_5OH-(H_2O)_n]^{\bullet+}$ have size dependency. The proton affinity of the acceptor moieties $(H_2O)_n$ becomes large as "n" increases, which leads to the proton transfer at the $n \geq 3$ cluster ion. The threshold value for the proton transfer from the phenol cation radical is predicted to lie at PA = 207 kcal/mol with the B3LYP method. This value is very reasonable, because the calculated energy difference between the phenol cation radical and the phenoxy π radical is 208 kcal/mol with the B3LYP method. The experimentally suggested threshold value of the proton transfer in this system is PA = 204.7 kcal/mol,[7] which is in good agreement with the calculated value. The present study by using the B3LYP density functional method not only well describes the experimental IR spectra but also predicts the stabilization energies and the most stable structures of the hydrogen-bonded cluster ions, $[C_6H_5OH-(H_2O)_n]^{\bullet+}$ ($n = 1-4$) and $[C_6H_5OH-NH_3]^{\bullet+}$.

The theoretically obtained vibrational spectra suggest that the $n = 3$ cluster ion involves mainly the proton-transferred branched structure and the $n = 4$ cluster ion may be a mixture of the branched form and the ringed structure, by comparing with the experimental spectra.

Acknowledgment. We wish to thank Prof. N. Mikami and Dr. S. Sato for their helpful comments and discussions. We would like to express our thanks to Dr. H. Watanabe for giving us his data on the geometries of the neutral phenol−water clusters. This research was partly supported by Grants-in-Aid for the priority area (No. 04243102) by the Ministry of Education, Science, and Culture, Japan. The computations were carried out using the computer centers of the Institute for Molecular Science and the Nobeyama Radio Observatory.

References and Notes

(1) Mikami, N. *Bull. Chem. Soc. Jpn.* **1995**, *68*, 683.
(2) Stanley, R. J.; Castleman, A. W. *J. Chem. Phys.* **1991**, *94*, 7744.
(3) Tanabe, S.; Ebata, T.; Fujii, M.; Mikami, N. *Chem. Phys. Lett.* **1993**, *215*, 347.
(4) Ebata, T.; Mizuochi, N.; Watanabe, T.; Mikami, N. *J. Phys. Chem.* **1996**, *100*, 546.
(5) Watanabe, T.; Ebata, T.; Tanabe, S.; Mikami, N. *J. Chem. Phys.* **1996**, *105*, 408.
(6) Sato, S.; Ebata, T.; Mikami, N. *Spectrochimica Acta* **1994**, *50A*, 1413.
(7) Sato, S.; Mikami, N. *J. Phys. Chem.* **1996**, *100*, 4765.
(8) Sawamura, T.; Fujii, A.; Sato, S.; Ebata. T.; Mikami, N. *J. Phys. Chem.* **1996**, *100*, 8131.
(9) Mikami, N.; Sato, S.; Ishigaki, M. *Chem. Phys. Lett.* **1993**, *202*, 431.
(10) Steadman, J.; Syage, J. A. *J. Am. Chem. Soc.* **1991**, *113*, 6786.
(11) Mikami, N.; Sasaki, T.; Sato, S. *Chem. Phys. Lett.* **1991**, *180*, 431.
(12) Mikami, N.; Okabe, A.; Suzuki, I. *J. Phys. Chem.* **1988**, *92*, 1858.
(13) Møller, C.; Plesset, M. S. *Phys. Rev.* **1934**, *46*, 618.
(14) Becke, A. D. *J. Chem. Phys.* **1993**, *98*, 1372.
(15) Becke, A. D. *J. Chem. Phys.* **1993**, *98*, 5648.
(16) Lee, C.; Yang, W.; Parr, R. G. *Phys. Rev.* **1988**, *B37*, 785.
(17) Parr, R. G.; Yang, W. *Density Functional Theory of Atoms and Molecules*; Oxford University Press: Oxford, 1989.
(18) Huzinaga, S. *J. Chem. Phys.* **1965**, *42*, 1923.
(19) Dunning, T. H. *J. Chem. Phys.* **1970**, *53*, 2823.
(20) van Lenthe, J. H.; van Duijneveldt-van de Rijdt, J. G. C. M.; van Duijneveldt, F. B. In *Ab initio Method in Quantum Chemistry*; Lawley, K. P., Ed.; Wiley: New York, 1987, Part 2, p 558.
(21) Frisch, M. J.; Trucks, G. W.; Schlegel, H. B.; Gill, P. M. W.; Johnson, B. G.; Robb, M. A.; Cheeseman, J. R.; Keith, T.; Petersson, G. A.; Montgomery, J. A.; Raghavachari, K.; Al-Laham, M. A.; Zakrzewski, V. G.; Ortiz, J. V.; Foresman, J. B.; Cioslowski, J.; Stefanov, B. B.; Nanayakkara, A.; Challacombe, M.; Peng, C. Y.; Ayala, P. Y.; Chen, W.; Wong, M. W.; Andres, J. L.; Replogle, E. S.; Gomperts, R.; Martin, R. L.; Fox, D. J.; Binkley, J. S.; Defrees, D. J.; Baker, J.; Stewart, J. P.; Head-Gordon, M.; Gonzalez, C.; Pople, J. A. *GAUSSIAN 94*; Gaussian, Inc.: Pittsburgh, PA, 1995.
(22) Bist, H. D.; Brand, J. C. D.; Williams. D. R. *J. Mol. Spectrosc.* **1967**, *24*, 402.
(23) Evans, J. C. S*pectrochim. Acta* **1960**, *16*, 1382.

(24) Green, J. H. S.; Harrison, D. J.; W. Kynaston, W. *Spectrochim. Acta* **1971**, *27A*, 2199.
(25) Hartland, G. V.; Henson, B. F.; Venturo, V. A.; Felker, P. M. *J. Phys. Chem.* **1992**, *96*, 1164.
(26) Cabral, B. J. C.; Fonseca, R. G. B.; Martinho Simões, J. A. M. *Chem. Phys. Lett*. **1996**, *258*, 436.
(27) Michalska, D.; Bieńko, D. C.; Abkowicz-Bieńko, A. J.; Latajka, Z. *J. Phys. Chem.* **1996**, *100*, 17786.
(28) *CRC Handbook of Chemistry and Physics*, 78th ed.; Lide, D. R., Ed.; CRC Press: Boca Raton, FL, 1997.
(29) Fujii, A.; Sawamura, T.; Tanabe, S.; Ebata, T.; Mikami, N. *Chem. Phys. Lett.* **1994**, *225*, 104.
(30) Tripathi, G. N. R.; Schuler, R. H. *J. Chem. Phys*. **1984**, *81*, 113.
(31) Ward, B. *Spectrochim. Acta A.* **1967**, *24A*, 813.
(32) Pullin, D.; Andrews, L. J. *Mol. Struct*. **1982**, *95*, 181.
(33) Yu, H.; Goddard, J. D. *J. Mol. Struct. (THEOCHEM)* **1991**, *233*, 129.
(34) Takahashi, J.; Momose, T.; Shida, T. *Bull. Chem. Soc. Jpn*. **1994**, *67*, 964.
(35) Nwobi, O.; Higgins, J.; Zhou, X.; Liu, R. *Chem. Phys. Lett.* **1997**, *272*, 155.
(36) Schütz, M.; Bürgi, T.; Leutwyler, S.; Fischer, T. *J. Chem. Phys.* **1993**, *98*, 3763.
(37) Feller, D.; Feyereisen, M. W. J. *Comput. Chem.* **1993**, *14*, 1027.
(38) Dopfer, O.; Reiser, G.; Müller-Dethlefs, K.; Schlag, E. W.; Colson, S. D. *J. Chem. Phys.* **1994**, *101*, 974.
(39) Hobza, P.; Burcl, R.; Spirko, V.; Dopfer, O.; Müller-Dethlefs, K.; Schlag, E. W. *J. Chem. Phys*. **1994**, *101*, 990.
(40) Reiser, G.; Dopfer, O.; Linder, R.; Henri, G.; Müller-Dethlefs, K.; Schlag, E. W.; Colson, S. D. *Chem. Phys. Lett*. **1991**, *181*, 1.
(41) Sodupe, M.; Oliva, A.; Bertrán, J. *J. Phys. Chem.* **1997**, *101*, 9142.
(42) Watanabe, H.; Iwata, S. *J. Chem. Phys.* **1996**, *105*, 420.
(43) Meot-Ner (Mautner), M.; Sieck, L. W. *J. Am. Chem. Soc.* **1991**, *113*, 4448.
(44) Cunningham, A. J.; Payzant, J. D.; Kebarle, P. *J. Am. Chem. Soc.* **1972**, *94*, 7627.
(45) Kebarle, P.; Searles, S. K.; Zolla, A.; Scarborough, J.; Arshadi, M. *J. Am. Chem. Soc*. **1967**, *89*, 6393.
(46) Schiefke, A.; Deusen, C.; Jacoby, C.; Gerhards, M.; Schmitt, M.; Kleinermanns, K.; Hering, P. *J. Chem. Phys.* **1995**, *102*, 9197.
(47) Iwasaki, A.; Fujii, A.; Watanabe, T.; Ebata, T.; Mikami, N. *J. Phys. Chem.* **1996**, *100*, 16053.
(48) Bürgi, T.; Schütz, M.; Leutwyler, S. *J. Chem. Phys.* **1995**, *103*, 6350.
(49) Gerhards, M.; Kleinermanns, K. *J. Chem. Phys.* **1995**, *103*, 7392.
(50) Fujii, A.; Iwasaki, A.; Yoshida, K.; Ebata, T.; Mikami, N. *J. Phys. Chem.* **1997**, *101*, 1798.
(51) DeFrees, D. J.; McIver, R. T., Jr.; Hehre, W. J. *J. Am. Chem. Soc.* **1980**, *102*, 3334.
(52) Choi, J.-H.; Kuwata, K. T.; Haas, B.-M.; Cao, Y.; Johnson, M. S.; Okumura, M. *J. Chem. Phys.* **1994**, *100*, 7153.